Acta Oceanol. Sin., 2024, Vol. 43, No. 11, P. 26–33
https://doi.org/10.1007/s13131-024-2430-8
http://www.aosocean.com
E-mail: ocean2@hyxb.org.cn

Differential scavenging behavior of anthropogenic Pb revealed by sediment traps in the northern South China Sea basin

Weiying Li[1], Jingjing Zhang[1], Hongliang Li[1, 2, 3*], Shuh-Ji Kao[4, 5], Zezhou Wu[1], Xingju He[1], Lihua Ran[1], Martin G. Wiesner[1, 6], Jianfang Chen[1, 7*]

[1] Key Laboratory of Marine Ecosystem Dynamics, Second Institute of Oceanography, Ministry of Natural Resources, Hangzhou 310012, China

[2] Southern Marine Science and Engineering Guangdong Laboratory (Zhuhai), Zhuhai 519099, China

[3] Observation and Research Station of Yangtze River Delta Marine Ecosystems, Ministry of Natural Resources, Zhoushan 316021, China

[4] State Key Laboratory of Marine Environmental Science and College of Ocean and Earth Sciences, Xiamen University, Xiamen 361102, China

[5] State Key Laboratory of Marine Resource Utilization in South China Sea, Hainan University, Haikou 570228, China

[6] Institute of Geology, University of Hamburg, Hamburg 20146, Germany

[7] State Key Laboratory of Satellite Ocean Environment Dynamics, Second Institute of Oceanography, Ministry of Natural Resources, Hangzhou 310012, China

Received 15 November 2023; accepted 15 December 2023

Abstract

Trace metals emitted from human activities may have penetrated into the deep seas, and the underlying control mechanisms remain poorly understood. Sinking particles collected by moored time-series sediment traps from the northern South China Sea (NSCS) basin showed significant enrichment of anthropogenic aerosol Pb relative to lithogenic Fe. Total mass flux was primarily driven by seasonal primary production, and significant positive correlations were found between Pb/Fe flux and major biogenic components, indicating the crucial role of the biological pump in Pb/Fe scavenging in the water column. Notably, Pb exhibited 30–50 times higher affinity to biogenic components than Fe. A comparison was made between the enrichment factors of Fe and Pb in aerosols, euphotic particles, and sinking particles, which revealed that Pb exhibited significantly higher particle reactivity than Fe. This higher particle reactivity may encompass processes such as adsorption/desorption, bioaccumulation and decomposition release. The differential scavenging behavior of Pb suggested that the majority of Pb was rapidly scavenged in the euphotic zone and was preferentially released for accumulation in the twilight zone. This accumulation may further outflow through the Luzon Strait and result in the high dissolved Pb concentration observed in the subsurface water columns in both the NSCS and western Pacific Ocean. The rest of anthropogenic Pb in sinking particles tended to penetrate into deeper water layers and continue to be released below the twilight zone. These findings provide new insights into the biogeochemical cycling of trace metals originating from anthropogenic aerosols in marginal seas and serve as an example of the fate of other anthropogenic atmospheric pollutants.

Key words: anthropogenic aerosol, Pb, sinking particle, biological pump, northern South China Sea

Citation: Li Weiying, Zhang Jingjing, Li Hongliang, Kao Shuh-Ji, Wu Zezhou, He Xingju, Ran Lihua, Wiesner Martin G., Chen Jianfang. 2024. Differential scavenging behavior of anthropogenic Pb revealed by sediment traps in the northern South China Sea basin. Acta Oceanologica Sinica, 43(11): 26–33, doi: 10.1007/s13131-024-2430-8

1 Introduction

Human activities have significantly increased the release of trace metals into the atmosphere and the ocean. Among the trace metals, Pb (as a harmful toxin) is considered to represent a “global geophysical experiment”, demonstrating the striking effect humans have existed on the natural environment (Gamo, 2020). These activities, including vehicle emissions, coal combustion, metal smelting and other industrial emissions, contribute to the majority of Pb enrichment in the upper ocean, primarily through aerosol deposition (Li et al., 2012; Pinedo-González et al., 2020; Zhu et al., 2020; Zhang et al., 2022b). The deposited anthropogenic aerosol Pb is transferred to the mesopelagic/bathypelagic zone, would impact the ecosystems and the biogeochemical cycling of Pb in the deep ocean, especially in regions with high aerosol inputs (Mahowald et al., 2018). Due to a lack of observational data in the ocean, the transport behavior of Pb from the atmosphere to the deep ocean remains poorly understood.

Foundation item: The National Natural Science Foundation of China under contract No. 42106045; the Scientific Research Fund of the Second Institute of Oceanography, MNR under contract No. JB2208; the National Science Foundation for Post-doctoral Scientists of China under contract No. 2021M703793; the Project Fund of Southern Marine Science and Engineering Guangdong Laboratory (Zhuhai) under contract No. SML2021SP207; the National Natural Science Foundation of China under contract No. 42330412.
*Corresponding author, E-mail: lihongliang@sio.org.cn; jfchen@sio.org.cn

Marine sinking particles containing biogenic and lithogenic matter play a vital role in transporting materials from the surface to the deep ocean, thus can provide valuable information on the behavior of oceanic sinks of trace metals originating from anthropogenic aerosols. Prior sediment trap studies suggest that possible anthropogenic aerosol signals of various trace metals, such as V, Zn and Pb in sinking particles from the North Pacific Western Subarctic Gyre and Sargasso Sea (Jickells et al., 1984; Lamborg et al., 2008; Huang and Conte, 2009), and Cd, Cu, Ni, Zn in sinking particles of the norhtern South China Sea (NSCS) (Ho et al., 2009, 2011; Takano et al., 2020; Liao et al., 2021). A recent study showed that anthropogenic aerosol Zn can account for up to 90% of the total Zn in sinking particles at 3 500 m in the NSCS (Liao et al., 2021). Nevertheless, due to the limited available data on sinking particles and simultaneous measurements of major components and typical trace metals, the mechanistic understandings of the scavenging and transfer of anthropogenic Pb from the surface to the deep ocean remains unclear.

The South China Sea (SCS), the largest marginal sea in the North Pacific Ocean, receives a tremendous amount of atmospheric materials, including Asian-sourced dust and coastal countries-originated anthropogenic aerosols (Chen et al., 2023a). Current studies have already demonstrated that anthropogenic aerosols are the dominant source of dissolved and particulate trace metals in the NSCS surface waters (Ho et al., 2007, 2010), and spatial distributions of aerosol optical depth (AOD) differ seasonally (Lin et al., 2009; Chen et al., 2023a). Since monsoon-driven primary productivity is regarded as the main controlling factor influencing the total mass flux (TMS) of sinking particles in the SCS (Li et al., 2017; Zhang et al., 2019), a one-year time-series sediment trap was deployed in the NSCS basin to quantify the particulate trace metal fluxes (Al, Fe and Pb) and to examine the relationships of metal fluxes with the major components of sinking particles. This work aims to investigate the signals of anthropogenic Pb in sinking particles and gain a better understand of its scavenging behavior during transfer to the deep ocean.

2 Methods

2.1 *Sample processing and major components analyses*

Three time-series moored sediment traps (Mark 7G-21) were deployed at the SCS-N station (18.5°N, 116°E, bottom depth of 3 736 m) at approximately 1 000 m, 2 150 m and 3 200 m during a period from June 2009 to May 2010 (Fig. 1a). Twenty samples were collected at each depth with a cone area of 0.5 m^2 and a 16-day sampling interval for each cup (one sample was missing at 3 200 m). Before deployment, the acid-washed sample cups (Polypropylene, Nalgene) were filled with a brine solution containing guarantee reagent grade 35 g/L NaCl and 3.3 g/L $HgCl_2$ (Ran et al., 2015; Zhang et al., 2019). After recovering the traps, the sample cups were detached, sealed and then stored at 4℃ for later analysis.

The method for the analysis of major components [organic matter, $CaCO_3$, opal and lithogenic matter (LM)] in sinking particles is detailed by Lahajnar et al. (2007) and particulate organic carbon Ran et al. (2015). Total organic matter (OM) was derived from particulate organic carbon (POC)×1.8 (Müller et al., 1986). Briefly, an empirical equation (Honjo, 1996) was used to describe the relationship among these major components:

$$\text{Lithogenic matter flux} = \text{Total particle flux} - CaCO_3 \text{ flux} - \text{OM flux} - \text{opal flux}.$$

2.2 *Trace metal analyses*

Al, Fe and Pb contents were determined following Liao et al. (2021). Sinking particles were predigested with a 3 mL mixture of super pure HNO_3-HF (1:5, *v*/*v*) in PFA vials at 110℃ overnight on a hot plate in a fume hood in a clean laboratory. Then, the samples were evaporated to dryness at 110℃ on a hot plate. After drying, the samples were added to a 3 mL mixture of super pure HNO_3-HF (1:5, *v*/*v*) again and placed in a digestion tank to fully digest for 48 h in an oven at 190℃. Subsequently, a 3 mL mixture

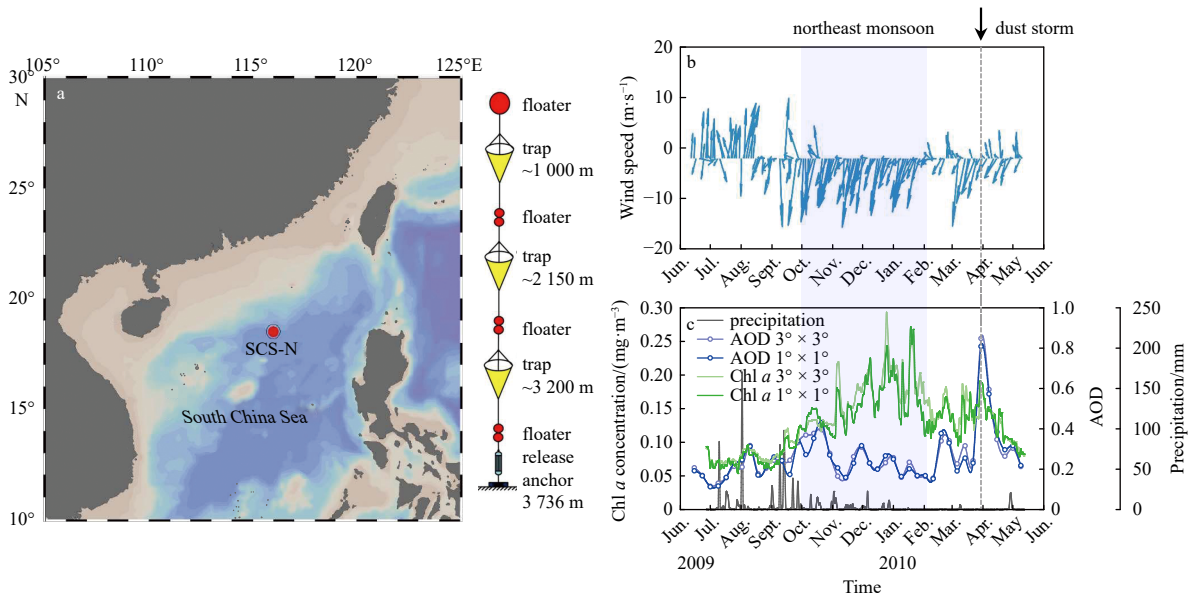

Fig. 1. The location of the SCS-N (18.5°N, 116°E, water depth 3 736 m) sediment trap mooring station in the northern South China Sea with the diagram of the three synchronized traps array structure to the right (a). The time-series of wind (b), 8-day average AOD, daily precipitation and surface Chl *a* data (c) at the SCS-N station during June 2009 to May 2010. Blue shade in b and c indicates northeast monsoon, the grey dashed line denotes the dust storm event in 19–21 March 2010.

of super pure 50% HCl and HNO_3 (4:1, *v/v*) was added to the digestion solution at 110℃ for 6 h, and then the solution was evaporated to dryness. To remove residual HF and HCl, the dried samples were redissolved in 3 mL of 50% ultrapure HNO_3 and evaporated to dryness at 110℃. Then, the dried samples were allowed to redissolve in 3 mL of 50% ultrapure HNO_3 again overnight at 110℃. Finally, the samples were diluted sequentially with 2% ultrapure HNO_3 for Pb analysis by inductively coupled plasma-mass spectrometry (ICP-MS, Thermo Fisher, iCAP-RQ). Al and Fe were measured by inductively coupled plasma-optical emission spectrometry (ICP-OES, Agilent 5110). The analytical precision was within 3% for the range of data presented.

The background concentrations of Al, Fe and Pb in the trap solution were basically below the detection limit or at low levels (ng/L), which were much lower than (at least two orders of magnitude) their concentrations in the final diluted samples of sinking particles, indicating negligible contamination from the brine solution.

2.3 *Remote-sensing and modeling data*

Daily wind and surface Chl *a* data were downloaded from the Copernicus Marine Service (https://marine.copernicus.eu/), with horizontal resolutions of 0.125° × 0.125° and 4 km × 4 km, respectively. The 8-day mean AOD data from MODIS-Aqua at 550 nm during the study period were downloaded from Giovanni (http://giovanni.gsfc.nasa.gov), with a 1° × 1° horizontal resolution. Daily precipitation data were obtained from the Asia-Pacific Data Research Center (http://apdrc.soest.hawaii.edu.), with a 0.67° × 1.25° horizontal resolution.

2.4 *Calculations and statistical analysis*

Al, as a popular lithogenic tracer, was strongly correlated with the lithogenic matter observed (Fig. S1,Table S2). Thus, we use Al content to calculate the enrichment factor (EF), which is widely used to characterize the predominant origins, e.g., natural or anthropogenic origins, of trace metals in various substances (aerosols, sinking particles and sediments) (Hsu et al., 2010; Xu et al., 2016; Conte et al., 2019). The EF value is described by the following equation:

$$\mathrm{EF} = \frac{[\mathrm{M}]/[\mathrm{Al}]_{\mathrm{particle}}}{[\mathrm{M}]/[\mathrm{Al}]_{\mathrm{crust}}},$$

where $[\mathrm{M}]/[\mathrm{Al}]_{\mathrm{particle}}$ is the concentration ratio of a given trace metal (M) to Al in sinking particles, and $[\mathrm{M}]/[\mathrm{Al}]_{\mathrm{crust}}$ is the concentration ratio of a given trace metal (M) to Al in the average crustal abundance (Hu and Gao, 2008). Generally, an EF value >2 is considered to indicate a significant effect of human activities.

Pearson's correlation coefficient square (R^2) was utilized to investigate the relationships between the fluxes of Al, Fe, Pb and particle major components, using a significance level of $p < 0.05$.

3 Results and discussion

3.1 *Seasonal atmospheric deposition and downward export of Fe and Pb via sinking particles*

As shown in Figs 1b and c, during our trap sampling period, the average wind speed was (7.0 ± 3.3) m/s, ranging from 1.2 m/s to 15.4 m/s, with the northeast monsoon prevailing from October 2009 to early February 2010, and the southwest monsoon prevailing from June to August 2009. Aerosol loading was expected to be higher during the northeast monsoon period due to long range transport. However, the 8-day mean AOD (1° × 1° and 3° × 3°) data did not reveal high values within our study area. At the end of March 2010, a significant peak appeared due to the invasion of a strong Asian dust storm (Wang et al., 2012). Precipitation, which can efficiently remove aerosols, was much less in winter and spring than in summer and autumn. In contrast, surface Chl *a* (1° × 1° and 3° × 3°) displayed a significant seasonal pattern with a strong and sustained peak during the northeast monsoon period. Previous studies have discussed that the higher primary productivity observed in winter can be attributed to intensive mixing and prominent nutrient supply caused by the northeast monsoon and surface cooling, while the lower surface Chl *a* observed may be limited by the nutrient supply due to the strong stratification that occurs during the weaker southwest monsoon (Ran et al., 2015; Tan et al., 2020). Overall, during our sampling period, rainfall in summer did not stimulate productivity as shown by surface Chl *a* and the low AOD in winter suggested that enhanced productivity was mainly caused by persistent unidirectional wind-induced nutrient supply.

The fluxes of total mass, Al, Fe and Pb (Figs 2a–d, Table S1) at each depth were generally higher in November 2009 to May 2010 (defined as the high particle flux period) than months from July to October 2010 (defined as the low particle flux period). This seasonal pattern was basically consistent with surface Chl *a*, indicating that sinking particle fluxes at SCS-N station are primarily driven by primary production. A similar pattern of sinking particles fluxes is observed at the Southeast Asian Time-series Study (SEATS) station (18°N, 116°E) near our study site (Ho et al., 2011; Liao et al., 2021). The average mass fluxes of Al, the most abundant trace element in sinking particles, were approximately two times higher than the fluxes of Fe at all depths. The average mass fluxes of Fe were (2.7 ± 2.2) mg/(m²·d), (3.3 ± 1.8) mg/(m²·d) and (3.2 ± 1.3) mg/(m²·d) at 1 000 m, 2 150 m and 3 200 m, respectively. These values were comparable with those data reported at the SEATS station (Ho et al., 2011). The average mass fluxes of Pb were two orders of magnitude lower than those of Al and Fe, with average values of (4.9 ± 2.5) μg/(m²·d), (5.6 ± 2.6) μg/(m²·d) and (5.0 ± 1.5) μg/(m²·d) at 1 000 m, 2 150 m and 3 200 m, respectively. Worthwhile to note that surface Chl *a* increased continuously from September until early February, but for the 1 000 m trap the Al, Fe and Pb fluxes increased dramatically in late October, peaked in in late November and then decreased gradually. During the early stage of the northeast monsoon, these peaks showed a one-month lag time as the depth increased while during the dust event the peaks appeared synchronously in the 1 000 and 2 150 m traps and disappeared in 3 200 m. This is in accordance with the previously estimated sinking rates of 30–50 m/d from the sea surface to a 1 000 m depth in the NSCS, and 50–100 m/d during an Asian dust event (Ran et al., 2015). The inconsistency in temporal patterns among AOD, Chl *a* and trace metal fluxes at the same site within 3° × 3° warrants explanation.

3.2 *Sources of Fe and Pb in sinking particles in the NSCS*

The $\mathrm{EF_{Fe}}$ in all samples were relatively uniform throughout the sampling period, with no significant seasonal variations (Fig. 2e). The average $\mathrm{EF_{Fe}}$ of all three trap depths was 1.2 ± 0.1, ranging from 1.1 to 1.5, which was very close to 1. Additionally, a strong positive correlation was observed between Fe and Al flux, and the intercept approached zero (Fig. S1). These results indicated that Fe was predominantly derived from lithogenic material, which is consistent with previous studies on sinking particles (Huang and Conte, 2009; Ho et al., 2011; Conte et al., 2019; Pull-

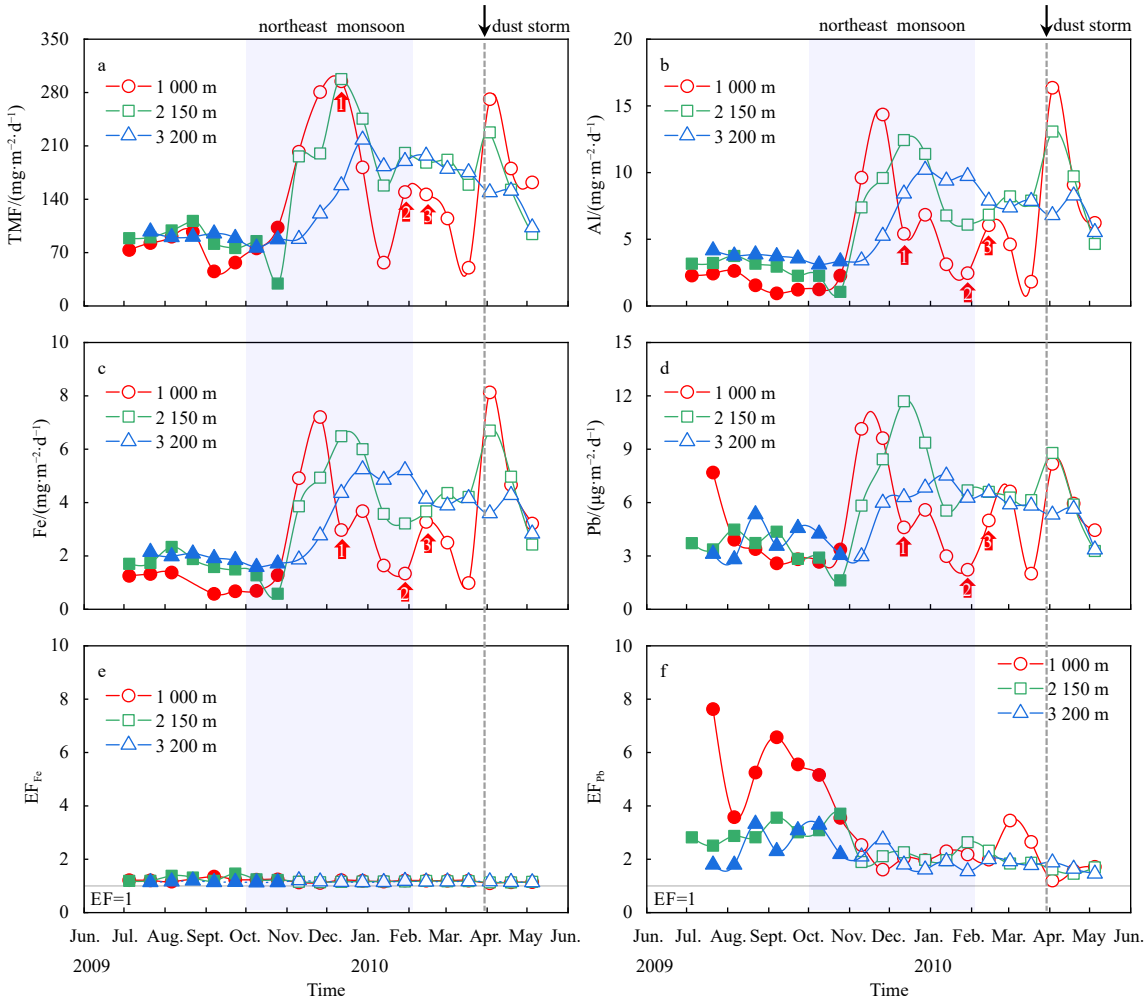

Fig. 2. The temporal variations of total mass flux (TMF) (a), Al flux (b), Fe flux (c), Pb flux (d), EF_{Fe} (e) and EF_{Pb} (f) of sinking particles. The date labels on the *x*-axis indicate the mid date of each sampling period. For all depths full and hollow symbol denote, respectively, the low and high particle flux period. The arrow with numbers 1, 2 and 3 represent the three uncommon samples with abnormal biogenic relationships.

wer and Waniek, 2020; Traill et al., 2022). In contrast, the correlation between Pb and Al fluxes was weaker than that of Fe and Al, and the intercept did not pass through zero (Fig. S1). The EF_{Pb} ranged between 1.2 and 7.6, with an average of 3.3 ± 1.9 at 1 000 m trap depth, which was higher than that of 2 150 m (p = 0.31) and 3 200 m (p < 0.05). The values at two deeper depths were averaged on 2.4 ± 0.6 and 2.1 ± 0.6, ranging from 1.5 to 3.7 and 1.5 to 3.3, respectively (Fig. 2f). At each trap depth, 79%, 70% and 40% of samples had EF_{Pb} values greater than 2, suggesting that anthropogenic sources contribute significantly to Pb flux in sinking particles, especially at that shallow and middle depths.

Since the SCS-N station is not affected by river discharge (Tan et al., 2020; Zhang et al., 2022a) and sinking particulate organic carbon for the entire water column is dominated by vertically settling fresh marine POC (84%–91%) with a small contribution from lateral transport (Zhang et al., 2022a), the most likely source of anthropogenic Pb is aerosol deposition. This inference is supported by multiple studies that highlight the significant impact of anthropogenic aerosols on dissolved Pb concentrations and isotope ratios in the marginal seas of China (Liao and Ho, 2018; Wu et al., 2018; Nakaguchi et al., 2021; Zhang et al., 2022b; Chen et al., 2023b), as well as recent concerns about the impact of fuel consumption for ship traffic on Pb pollution in marine shipping areas (Xie et al., 2022). In addition, the contribution of anthropogenic aerosol deposition to elements such as Cd, Cu, Ni and Zn in sinking particles in the NSCS has been confirmed (Ho et al., 2009, 2011; Takano et al., 2020; Liao et al., 2021).

Intriguingly, a noticeable asymmetric signature of Pb and EF_{Pb} was observed at all depths. This was characterized by low Pb flux but high EF_{Pb} during the low particle flux period and high Pb flux but low EF_{Pb} during the high particle flux period (Figs 2d and f). Unlike Fe, which had relatively uniform EF_{Fe}, the EF_{Pb} varied over time and vertical space for Pb, indicating that Pb behaves differently from Fe in sinking particles (Figs 2e and f).

3.3 *Vertically differential scavenging between Fe and Pb*

To investigate the vertical differential scavenging of Fe and Pb in the water column, we compared the vertical spatial distributions of EF_{Fe} and EF_{Pb} in this study with the data for reported aerosols, sinking particles (30 m, 100 m and 160 m) and sediments (Figs 3a and b).

In general, Fe was slightly enriched in sinking particles in the upper ocean (Fig. 3a). The vertical distribution of EF_{Fe} showed an extreme value in the euphotic zone due to the biological utilization of Fe, which is an essential micronutrient for phytoplankton, and then decreased in the twilight zone as a result of biogenic

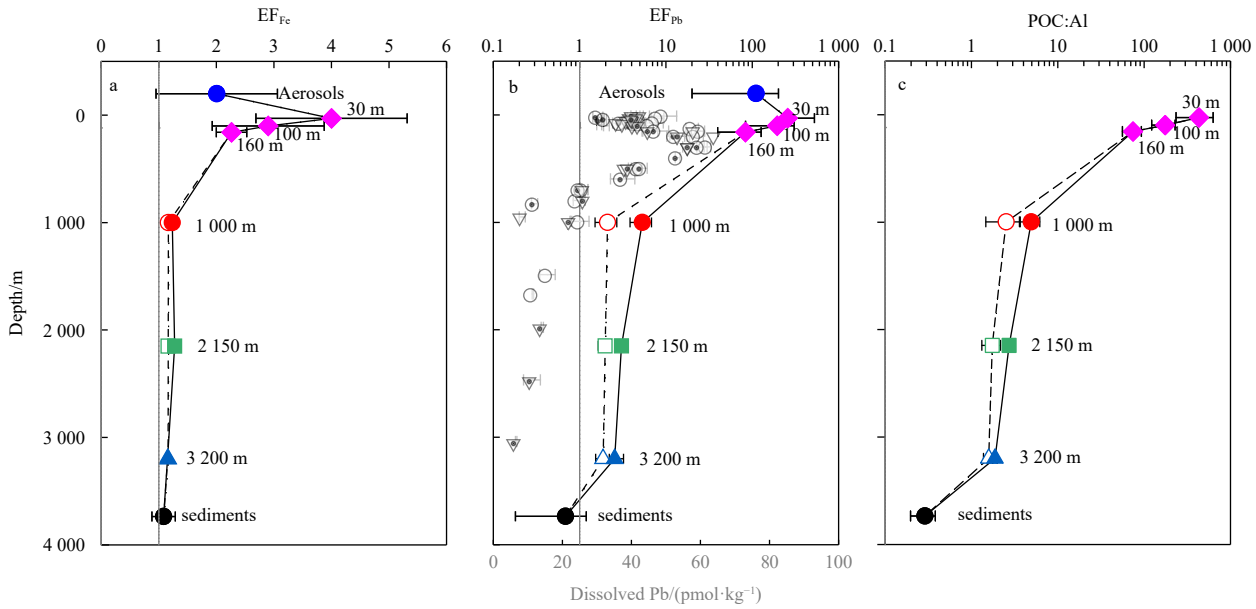

Fig. 3. The vertical distribution of EF_{Fe} (a), EF_{Pb} (b) and POC : Al molar concentration ratio (c). Full and hollow symbol stand, respectively, for the low and high particle flux period. The reference values of EF_{Fe} and EF_{Pb} were calculated by dividing the reported trace metal to Al ratios in aerosols, 30–160 m sinking particles and sediments by the trace metal to Al ratios in the average crustal abundance (Table S3). The reference values of POC : Al molar concentration ratio in 30–160 m sinking particles and sediments were also listed in Table S3. Dissolved Pb concentration data in b were collected from Kuroshio transect (Chen et al., 2023b).

matter decomposition. However, in the bathypelagic zone, the vertical profile of EF_{Fe} remained relatively constant (close to 1), similar to that in the sediments, implying an equilibrium of Fe removal.

Pb is a nonbioactive element; however, it can be adsorbed onto sinking particles due to its particle-reactive properties. As shown in Fig. 3b, when highly Pb-enriched anthropogenic aerosols settle, the intensity of Pb scavenging through adsorption and bioaccumulation (Noriki et al., 1985; Pohl et al., 2004) was two orders of magnitude greater than that of Fe in the euphotic zone. In the twilight zone, EF_{Pb} in sinking particles decreased dramatically from 160 m (83 ± 44) to 1 000 m (3.3 ± 1.9). The nearly parallel vertical distribution of EF_{Pb} and POC : Al in sinking particles suggested that Pb is scavenged onto organic matter (Figs 3b and c). In the twilight zone, with the intensification of organic particle decomposition, a large amount of Pb may be released from the particulate phase and accumulate in this layer. This could be one of the important reasons for explaining why the maximum concentration of dissolved anthropogenic Pb was found in the subsurface layer in regions with high aerosol inputs (Zhang et al., 2022b; Chen et al., 2023b). Based on the three-layered structure of the SCS (Wang et al., 2019) and a previous study suggesting that organic carbon can be exported into the adjacent North Pacific by the intermediate waters of the SCS (Dai et al., 2009), the accumulated dissolved Pb in the twilight zone may also outflow to the Pacific Ocean through the Luzon Strait.

Even though the majority of anthropogenic Pb was rapidly scavenged and released in the upper ocean, there was still a portion of anthropogenic Pb that could be transported to the deep ocean via sinking particles. Recently, researchers used dissolved Pb isotopes data and modeling to demonstrate that dissolved anthropogenic Pb can be transported from the upper to the deep Pacific Ocean by reversible scavenging within high-productivity stations (Lanning et al., 2023). In this study, anthropogenic Pb enrichment in sinking particles provided direct evidence of the possible exchange of dissolved and particulate anthropogenic Pb in the deep ocean. However, in contrast with the gradually decreased POC : Al during the low and high particle flux periods, EF_{Pb} exhibited two different trends at different levels of particle flux (Figs 3b and c). During the high particle flux period, EF_{Pb} remained relatively constant (EF_{Pb} equal to 2.1 ± 0.6, 2.0 ± 0.3, and 1.9 ± 0.3 at 1 000 m, 2 150 m and 3 200 m, respectively). During the low particle flux period, EF_{Pb} gradually decreased with depth (EF_{Pb} equal to 5.3 ± 1.5, 3.1 ± 0.4, and 2.5 ± 0.7 at 1 000 m, 2 150 m and 3 200 m, respectively). This distinguishing behavior of Pb, between low and high particle flux periods, needs to be investigated in more detail to better elucidate Pb scavenging throughout the entire water column.

3.4 *Biogenic matter facilitates the scavenging of Pb to the deep sea*

Biological mechanisms, including biological uptake and the use of biogenic particles as adsorbents, may be effective in removing trace metals originating from aerosols to the deep ocean (Ho et al., 2011; Liao et al., 2021). This proposed mechanism is currently based on the observation that the bioessential trace metal to P ratios in sinking particles are much higher than their intracellular quotas in surface waters (Ho et al., 2011) and the correlation between trace metals and P or organic-C (Takano et al., 2020). In fact, the transport of anthropogenic aerosol trace metals in sinking particles is complex, involving the production and remineralization of biogenic particles, the increase and accumulation of lithogenic particles and reversible scavenging differences in the high or low particle flux periods (Jickells et al., 1990; Lam and Marchal, 2015; Lanning et al., 2023).

In our study, in both the low and high particle flux periods, of the four major components of sinking particles, the flux of Fe was most strongly correlated with the flux of lithogenic matter (R^2 = 0.95), as expected, but it was also closely related to opal (R^2 = 0.82), organic matter (R^2 = 0.75), and $CaCO_3$ (R^2 = 0.56) (Fig. S2). These result suggest that while the particulate flux of Fe is pre-

dominantly controlled by lithogenic matter (account for 29.9% ± 8.7% of the total sinking particles), biogenic carrier materials can also contribute significantly. The flux of Pb exhibited the strongest correlation with the flux of organic matter (R^2 = 0.77), followed by opal, lithogenic matter and $CaCO_3$ (R^2 equal to 0.72, 0.70 and 0.58, respectively), implying that the coupling and transport of anthropogenic Pb were primarily regulated by organic matter, that is, biological control. Since biogenic matter as the bulk component of sinking particles (account for 70.1% ± 8.7% of the total sinking particles) can adsorb lithogenic and anthropogenic particles, the above significant relationships Fig. S3 (p < 0.000 1) suggested that the biological pump could play an important role in anthropogenic Pb scavenging in the water column.

Furthermore, EF_{Fe} was only slightly affected by an increase in the flux of major components (Fig. S3). This indicated that Fe in sinking particles at all three sampling depths originated primarily from a stable lithogenic source derived from the crust, including atmospheric dust deposition, sediment resuspension, lateral advection of suspended clay particles, and other lithogenic particles from ocean margins (Liu et al., 2014; Zhang et al., 2019; Kim et al., 2020). For anthropogenic Pb, EF_{Pb} tended to be constant with increasing flux of the four major components, implying that any increase in material flux will dilute the signal of Pb, particularly lithogenic matter flux (Fig. S3). The EF_{Pb} of 1.2 after the dust storm event can also reflect the dilution effect due to the input of a large amount of lithogenic material (Fig. 2f). Combined with the biological control, we hypothesized that EF_{Pb} in sinking particles is primarily controlled by the interaction of biogenic enrichment and lithogenic dilution.

In fact, as shown in Fig. 4, the relatively uniform EF_{Fe} values showed slightly positive correlations with OM : LM, opal : LM and $CaCO_3$: LM ratios, while EF_{Pb} displayed significantly positive correlations (R^2 equal to 0.78, 0.65 and 0.52 respectively, all p < 0.000 1). Based on their correlations, we found that Pb exhibited 30–50 times higher affinity to biogenic components than Fe, further indicating that the downward transport of anthropogenic Pb was regulated by biogenic components. Except that the three uncommon samples with abnormal biogenic relationships (Figs 2, 4 and S2), which may be affected by the low anthropogenic Pb supply. More specifically, we observed that the higher EF_{Pb} values were associated with higher ratios of biogenic matter (organic matter, opal and $CaCO_3$) to lithogenic matter at each depth during the low particle flux period (Fig. 4). This confirms our hypothesis that biogenic enrichment superimposed by lithogenic dilution results in differential Pb scavenging behavior in space and time. Although marine primary productivity was much higher in the high particle flux period and the adsorption of substantial lithogenic matter can increase total flux, forming a "ballast effect", it would also dilute biogenic components and decrease the Pb enrichment signals. In contrast, the lower primary productivity but purer biological processes emphasized the role of the biological pump in scavenging Pb during the low particle flux period. This unique differential scavenging pattern of Pb in the NSCS contributes to a better understanding of the biogeochemical cycling of trace metals originating from anthropogenic aerosols in the water column.

4 Conclusions

In this study, the sources, seasonal and vertical variability, and enrichment of Fe and Pb in sinking particles were investigated in the NSCS. The results showed that Fe was predominantly of lithogenic origin, whereas Pb had strong anthropogenic aerosol contributions. Seasonal variability analysis showed that the fluxes of total mass and Pb/Fe were mainly driven by primary production. The vertical distribution of EF_{Pb} and EF_{Fe} revealed that Pb has a higher intensity of downward scavenging onto organic matter compared to Fe in the euphotic zone, and may accumulate in the twilight zone due to the decomposition of organic particles. Additionally, the fluxes of Pb/Fe were strongly correlated with major biogenic components, and Pb exhibited 30–50

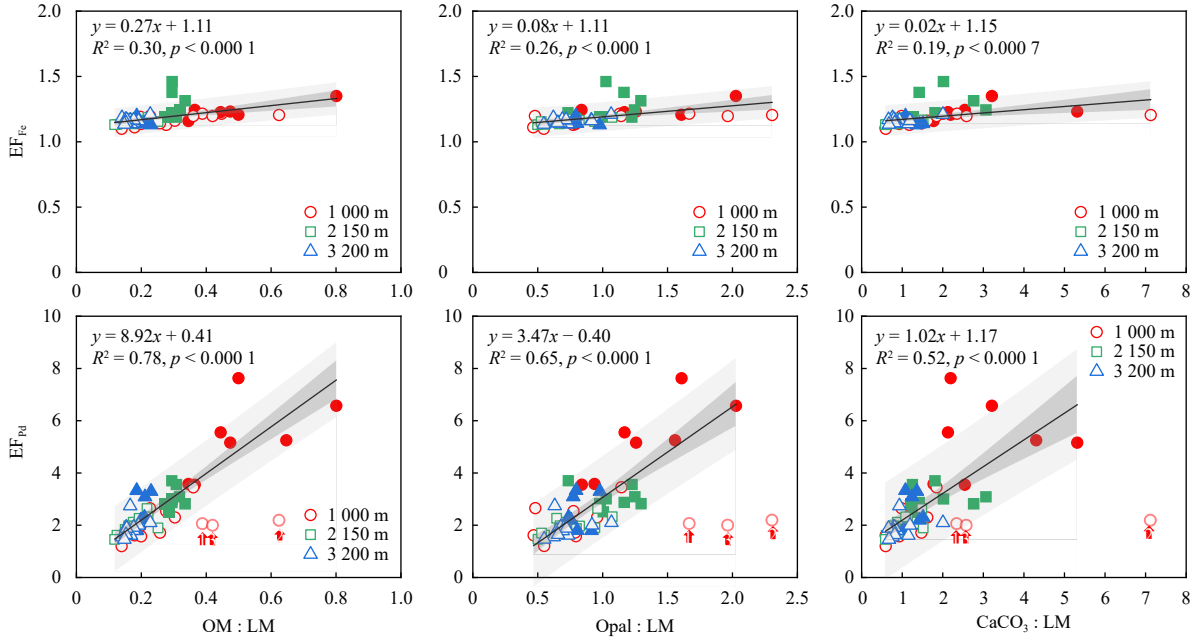

Fig. 4. Correlation between the EF_{Fe}, EF_{Pb} and the ratios of OM : LM, Opal : LM, and $CaCO_3$: LM, respectively. OM and LM represent organic matter and lithogenic matter, respectively. Full and hollow symbol denote, respectively, the low and high particle flux period. The arrow numbers 1, 2 and 3 represent the three uncommon samples with abnormal biogenic relationships. Shades of dark grey and light grey represent 95% confidence band and prediction band, respectively.

times higher affinity for biogenic components than Fe, highlighting the biological control on Pb scavenging. With increasing and sustained inputs of anthropogenic aerosols in the NSCS, the accumulation of dissolved anthropogenic Pb in the twilight zone could potentially extend from the SCS to the Pacific Ocean, while the scavenging of Pb by biogenic matter will also have an ongoing impact on the deep sea.

Acknowledgements

We thank Jihao Zhu (Key Laboratory of Submarine Geosciences, Second Institute of Oceanography, Ministry of Natural Resources) and Yaojin Chen (State Key Laboratory of Marine Environmental Science, Xiamen University) for technical assistance with Al, Fe and Pb measurements. We would also like to thank Wen-Hsuan Liao, Li Luo and the other two anonymous reviewers for their valuable and constructive comments on this manuscript.

References

Chen Mengli, Boyle E A, Jiang Shuo, et al. 2023b. Dissolved Lead (Pb) concentrations and pb isotope ratios along the East China Sea and Kuroshio transect—evidence for isopycnal transport and particle exchange. Journal of Geophysical Research: Oceans, 128(2): e2022JC019423, doi: 10.1029/2022JC019423

Chen Jie, Zhu Wenyue, Liu Qiang, et al. 2023a. Temporal evolution and regional properties of aerosol over the South China Sea. Remote Sensing, 15(2): 501, doi: 10.3390/rs15020501

Conte M H, Carter A M, Koweek D A, et al. 2019. The elemental composition of the deep particle flux in the Sargasso Sea. Chemical Geology, 511: 279–313, doi: 10.1016/j.chemgeo.2018.11.001

Dai Minhan, Meng Feifei, Tang Tiantian, et al. 2009. Excess total organic carbon in the intermediate water of the South China Sea and its export to the North Pacific. Geochemistry, Geophysics, Geosystems, 10(12): Q12002

Gamo T. 2020. Anthropogenic lead pollution in the ocean. In: Himiyama Y, Satake K, Oki T, eds. Human Geoscience. Singapore: Springer, 295–306

Ho Tung-Youan, Chou Wenchen, Lin Huiling, et al. 2011. Trace metal cycling in the deep water of the South China Sea: the composition, sources, and fluxes of sinking particles. Limnology and Oceanography, 56(4): 1225–1243, doi: 10.4319/lo.2011.56.4.1225

Ho Tung-Youan, Chou Wenchen, Wei Ching-Ling, et al. 2010. Trace metal cycling in the surface water of the South China Sea: vertical fluxes, composition, and sources. Limnology and Oceanography, 55(5): 1807–1820, doi: 10.4319/lo.2010.55.5.1807

Ho Tung-Youan, Wen Liang-Saw, You Chen-Feng, et al. 2007. The trace metal composition of size-fractionated plankton in the South China Sea: biotic versus abiotic sources. Limnology and Oceanography, 52(5): 1776–1788, doi: 10.4319/lo.2007.52.5.1776

Ho Tung-Youan, You Chen-Feng, Chou Wen-Chen, et al. 2009. Cadmium and phosphorus cycling in the water column of the South China Sea: the roles of biotic and abiotic particles. Marine Chemistry, 115(1–2): 125–133, doi: 10.1016/j.marchem.2009.07.005

Honjo S. 1996. Fluxes of particles to the interior of the open oceans. In: Ittekkot V, Schaefer P, Honjo S, et al., eds. Particle Flux in the Ocean. New York: John Wiley & Sons, 372

Hsu Shih-Chieh, Wong George T F, Gong Gwo-Ching, et al. 2010. Sources, solubility, and dry deposition of aerosol trace elements over the East China Sea. Marine Chemistry, 120(1–4): 116–127, doi: 10.1016/j.marchem.2008.10.003

Hu Zhaochu, Gao Shan. 2008. Upper crustal abundances of trace elements: a revision and update. Chemical Geology, 253(3–4): 205–221, doi: 10.1016/j.chemgeo.2008.05.010

Huang S, Conte M H. 2009. Source/process apportionment of major and trace elements in sinking particles in the Sargasso Sea. Geochimica et Cosmochimica Acta, 73(1): 65–90, doi: 10.1016/j.gca.2008.08.023

Jickells T D, Deuser W G, Fleer A, et al. 1990. Variability of some elemental fluxes in the western tropical Atlantic Ocean. Oceanologica Acta, 13: 291–298

Jickells T D, Deuser W G, Knap A H. 1984. The sedimentation rates of trace elements in the Sargasso Sea measured by sediment trap. Deep-Sea Research Part A: Oceanographic Research Papers, 31(10): 1169–1178

Kim M, Hwang J, Eglinton T I, et al. 2020. Lateral particle supply as a key vector in the oceanic carbon cycle. Global Biogeochemical Cycles, 34(9): e2020GB006544, doi: 10.1029/2020GB006544

Lahajnar N, Wiesner M G, Gaye B. 2007. Fluxes of amino acids and hexosamines to the deep South China Sea. Deep-Sea Research Part I: Oceanographic Research Papers, 54(12): 2120–2144, doi: 10.1016/j.dsr.2007.08.009

Lam P J, Marchal O. 2015. Insights into particle cycling from thorium and particle data. Annual Review of Marine Science, 7: 159–184, doi: 10.1146/annurev-marine-010814-015623

Lamborg C H, Buesseler K O, Lam P J. 2008. Sinking fluxes of minor and trace elements in the North Pacific Ocean measured during the VERTIGO program. Deep-Sea Research Part II: Topical Studies in Oceanography, 55(14–15): 1564–1577, doi: 10.1016/j.dsr2.2008.04.012

Lanning N T, Jiang Shuo, Amaral V J, et al. 2023. Isotopes illustrate vertical transport of anthropogenic Pb by reversible scavenging within Pacific Ocean particle veils. Proceedings of the National Academy of Sciences of the United States of America, 120(23): e2219688120

Li Qian, Cheng Hongguang, Zhou Tan, et al. 2012. The estimated atmospheric lead emissions in China, 1990–2009. Atmospheric Environment, 60: 1–8, doi: 10.1016/j.atmosenv.2012.06.025

Li Hongliang, Wiesner M G, Chen Jianfang, et al. 2017. Long-term variation of mesopelagic biogenic flux in the central South China Sea: impact of monsoonal seasonality and mesoscale eddy. Deep-Sea Research Part I: Oceanographic Research Papers, 126: 62–72, doi: 10.1016/j.dsr.2017.05.012

Liao Wen-Hsuan, Ho Tung-Yuan. 2018. Particulate trace metal composition and sources in the Kuroshio adjacent to the East China Sea: the importance of aerosol deposition. Journal of Geophysical Research: Oceans, 123(9): 6207–6223, doi: 10.1029/2018JC014113

Liao Wen-Hsuan, Takano S, Tian Hung-An, et al. 2021. Zn elemental and isotopic features in sinking particles of the South China Sea: implications for its sources and sinks. Geochimica et Cosmochimica Acta, 314: 68–84, doi: 10.1016/j.gca.2021.09.013

Lin I I, Wong George T F, Lien Chun-Chi, et al. 2009. Aerosol impact on the South China Sea biogeochemistry: an early assessment from remote sensing. Geophysical Research Letters, 36(17): L17605

Liu Jianguo, Clift P D, Yan Wen, et al. 2014. Modern transport and deposition of settling particles in the northern South China Sea: sediment trap evidence adjacent to Xisha Trough. Deep-Sea Research Part I: Oceanographic Research Papers, 93: 145–155, doi: 10.1016/j.dsr.2014.08.005

Müller P J, Suess E, AndréUngerer C. 1986. Amino acids and amino sugars of surface particulate and sediment trap material from waters of the Scotia Sea. Deep-Sea Research Part A: Oceanographic Research Papers, 33(6): 819–838

Mahowald N M, Hamilton D S, Mackey K R M, et al. 2018. Aerosol trace metal leaching and impacts on marine microorganisms. Nature Communications, 9(1): 2614, doi: 10.1038/s41467-018-04970-7

Nakaguchi Y, Ikeda Y, Sakamoto A, et al. 2021. Distribution and stoichiometry of Al, Mn, Fe, Co, Ni, Cu, Zn, Cd, and Pb in the East China Sea. Journal of Oceanography, 77(3): 463–485, doi: 10.1007/s10872-020-00577-z

Noriki S, Ishimori N, Harada K, et al. 1985. Removal of trace metals from seawater during a phytoplankton bloom as studied with sediment traps in Funka Bay, Japan. Marine Chemistry, 17(1): 75–89, doi: 10.1016/0304-4203(85)90037-4

Pinedo-González P, Hawco N J, Bundy R M, et al. 2020. Anthropogenic Asian aerosols provide Fe to the North Pacific Ocean. Proceedings of the National Academy of Sciences of the United States of America, 117(45): 27862–27868

Pohl C, Löffler A, Hennings U. 2004. A sediment trap flux study for trace metals under seasonal aspects in the stratified Baltic Sea (Gotland Basin; 57°19.20′N; 20°03.00′E). Marine Chemistry, 84(3–4): 143–160, doi: 10.1016/j.marchem.2003.07.002

Pullwer J, Waniek J J. 2020. Particulate trace metal fluxes in the center of an oceanic desert: Northeast Atlantic subtropical gyre. Journal of Marine Systems, 212: 103447, doi: 10.1016/j.jmarsys.2020.103447

Ran Lihua, Chen Jianfang, Wiesner M G, et al. 2015. Variability in the abundance and species composition of diatoms in sinking particles in the northern South China Sea: results from time-series moored sediment traps. Deep-Sea Research Part II: Topical Studies in Oceanography, 122: 15–24, doi: 10.1016/j.dsr2.2015.07.004

Takano S, Liao Wen-Hsuan, Tian Hung-An, et al. 2020. Sources of particulate Ni and Cu in the water column of the northern South China Sea: evidence from elemental and isotope ratios in aerosols and sinking particles. Marine Chemistry, 219: 103751, doi: 10.1016/j.marchem.2020.103751

Tan Shiru, Zhang Jingjing, Li Hongliang, et al. 2020. Deep ocean particle flux in the Northern South China Sea: variability on intra-seasonal to seasonal timescales. Frontiers in Earth Science, 8: 74, doi: 10.3389/feart.2020.00074

Traill C D, Weis J, Wynn-Edwards C, et al. 2022. Lithogenic particle flux to the subantarctic Southern Ocean: a multi-tracer estimate using sediment trap samples. Global Biogeochemical Cycles, 36(9): e2022GB007391, doi: 10.1029/2022GB007391

Wang Sheng-Hsiang, Christina Hsu N, Tsay S C, et al. 2012. Can Asian dust trigger phytoplankton blooms in the oligotrophic northern South China Sea?. Geophysical Research Letters, 39(5): L05811

Wang Dongxiao, Wang Qiang, Cai Shuqun, et al. 2019. Advances in research of the mid-deep South China Sea circulation. Science China: Earth Sciences, 62(12): 1992–2004, doi: 10.1007/s11430-019-9546-3

Wu Yunchao, Zhang Jingping, Ni Zhixin, et al. 2018. Atmospheric deposition of trace elements to Daya Bay, South China Sea: fluxes and sources. Marine Pollution Bulletin, 127: 672–683, doi: 10.1016/j.marpolbul.2017.12.046

Xie Sirong, Jiang Wei, Sun Yinan, et al. 2022. Interannual variation and sources identification of heavy metals in seawater near shipping lanes: evidence from a coral record from the northern South China Sea. Science of the Total Environment, 854: 158755

Xu Fangjian, Tian Xu, Yin Feng, et al. 2016. Heavy metals in the surface sediments of the northern portion of the South China Sea shelf: distribution, contamination, and sources. Environmental Science and Pollution Research, 23(9): 8940–8950, doi: 10.1007/s11356-016-6151-1

Zhang Jingjing, Li Hongliang, Wiesner M G, et al. 2022a. Carbon isotopic constraints on basin-scale vertical and lateral particulate organic carbon dynamics in the northern South China Sea. Journal of Geophysical Research: Oceans, 127(8): e2022JC018830, doi: 10.1029/2022JC018830

Zhang Jingjing, Li Hongliang, Xuan Jiliang, et al. 2019. Enhancement of mesopelagic sinking particle fluxes due to upwelling, aerosol deposition, and monsoonal influences in the Northwestern South China Sea. Journal of Geophysical Research: Oceans, 124(1): 99–112, doi: 10.1029/2018JC014704

Zhang Ruifeng, Ren Jingling, Zhang Zhaoru, et al. 2022b. Distribution patterns of dissolved trace metals (Fe, Ni, Cu, Zn, Cd, and Pb) in China marginal seas during the GEOTRACES GP06-CN cruise. Chemical Geology, 604: 120948, doi: 10.1016/j.chemgeo.2022.120948

Zhu Chuanyong, Tian Hezhong, Hao Jiming. 2020. Global anthropogenic atmospheric emission inventory of twelve typical hazardous trace elements, 1995–2012. Atmospheric Environment, 220: 117061, doi: 10.1016/j.atmosenv.2019.117061

Supplementary information:

Fig. S1. The cross correlations of LM, Fe and Pb flux with Al flux.

Fig. S2. Correlation of Fe and Pb flux with major components (organic matter, opal, $CaCO_3$ and lithogenic matter) flux in sinking particles.

Fig. S3. Correlation of EF_{Fe} and EF_{Pb} with major components (organic matter, opal, $CaCO_3$ and lithogenic matter) flux in sinking particles.

Table S1. The raw data of the Al, Fe and Pb fluxes at 1 000 m, 2 150 m and 3 200 m in sinking particles.

Table S2. The concentrations, estimated fluxes of Al, Fe and Pb and the ratios of Fe:Al and Pb:Al in aerosols collected from cities, island and marginal seas around China.

Table S3. The ratios of Fe:Al and Pb:Al in reported aerosols, sinking particles (30 m, 100 m and 160 m), sediments and crust, and the ratios of POC:Al in reported sinking particles (30 m, 100 m and 160 m) and sediments.

The supplementary information is available online at https://doi.org/10.1007/s13131-024-2430-8 and http://www.aosocean.com/. The supplementary information is published as submitted, without typesetting or editing. The responsibility for scientific accuracy and content remains entirely with the authors.